

Modeling soil organic carbon with Quantile Regression: Dissecting predictors' effects on carbon stocks

Luigi Lombardo^{1,2*}, Sergio Saia³, Calogero Schillaci⁴, P. Martin Mai²,
Raphaël Huser¹

¹ Computer, Electrical and Mathematical Sciences & Engineering Division, KAUST,
Thuwal, Saudi Arabia

² Physical Sciences and Engineering Division, KAUST, Thuwal, Saudi Arabia

³Council for Agricultural Research and Economics (CREA)

Cereal and Industrial Crops Research Centre (CREA-CI), Foggia, Italy

⁴Department of Agricultural and Environmental Science, University of Milan, Italy

August 15, 2017

Abstract

Soil Organic Carbon (SOC) estimation is crucial to manage both natural and anthropic ecosystems and has recently been put under the magnifying glass after the Paris agreement 2016 due to its relationship with greenhouse gas. Statistical applications have dominated the SOC stock mapping at regional scale so far. However, the community has hardly ever attempted to implement Quantile Regression (QR) to spatially predict the SOC distribution. In this contribution, we test QR to estimate SOC stock (0-30 *cm* depth) in the agricultural areas of a highly variable semi-arid region (Sicily, Italy, around 25,000 *km*²) by using topographic and remotely sensed predictors. We also compare the results with those from available SOC stock measurement. The QR models produced robust performances and allowed to recognize dominant effects among the predictors with respect to the considered quantile. This information, currently lacking, suggests that QR can discern predictor influences on SOC stock at specific sub-domains of each predictors. In this work, the predictive map generated at the median shows lower errors than those of the Joint Research Centre and International Soil Reference, and Information Centre benchmarks. The results suggest the use of QR as a comprehensive and effective method to map SOC using legacy data in agro-ecosystems. The R code scripted in this study for QR is included.

Keywords: Quantile Regression, R coding, Topsoil Organic Carbon, Digital Soil Mapping, Mediterranean agro-ecosystem

Corresponding Author: Luigi Lombardo*, Email: luigi.lombardo83@gmail.com

1 Introduction

Soil Organic Carbon (SOC) plays a key role in various agricultural and ecological processes related to soil fertility, carbon cycle and soil-atmosphere interactions including CO₂ sequestration. Thus, its knowledge has a crucial importance both at global and local scales, especially when aiming at managing natural, anthropic areas and especially agricultural lands. In this context, the scientific community has spent considerable efforts in mapping SOC, modeling its spatiotemporal variation and confirming its primary role in shaping ecosystems functioning [Ajami et al., 2016, Grinand et al., 2017, Ratnayake et al., 2014, Schillaci et al., 2017a].

Spatiotemporal studies can be found in various geographic contexts from Africa [Akpa et al., 2016], Asia [Chen et al., 2016], Australia [Henderson et al., 2005], Europe [Yigini and Panagos, 2016], North-America [West and Wali, 2002] to South-America [Araujo et al., 2016]. The variability of the local landscape, available funding, mean gross income of the population in the area and temporal commitment affect the number of samples, their spatial density and distribution. As a result, there are experiments conducted on almost regular and dense grids, most of which focus on small areas [Lacoste et al., 2014, Taghizadeh-Mehrjardi et al., 2016] and other where the sampling strategy significantly varies across space [Mondal et al., 2016]. The latter studies mainly correspond to regional or even greater scales [Reijneveld et al., 2009, Sreenivas et al., 2016], with only few cases where an optimal sample density is maintained at a national level [Mulder et al., 2016]. The characteristics of environment under study can require the use of different predictors capable of explaining the variability of soil traits, topography and standing biocoenosis, especially (cropped or natural) phytocoenosis, the latter being efficiently explained by remotely sensed (RS) properties [Morellos et al., 2016, Peng et al., 2015].

Modeling procedures for SOC primarily aims at constructing present, past or predictive maps and studying the role of each predictor over the target variable. Regarding the latter, the estimation of predictor contributions on a target variable such as SOC, is of particular interest to efficiently obtain agro-environmental and social benefits [e.g. Rossel and Bouma, 2016].

Statistical applications provide quantitative ways to deal with such research questions. The current literature encompasses algorithms that can be clustered into interpolative and predictive. Pure interpolators are broadly used when the density of the samples is sufficient to regularly describe the variation of SOC across a given area. Examples can be found [Hoffmann et al., 2014, Piccini et al., 2014] with excellent performances reported. The weakness of these approaches becomes evident when using data sets with non-regular distribution in space [Dai et al., 2014, Miller et al., 2016]. Conversely, regression-based predictive models hardly suffer from the spatial sampling scheme as they do not rely on the distribution across the geographic space in order to derive functional relations between SOC and dependent variables [Hobley et al., 2016].

Among these, linear regression models are a well-established tool for estimating how, on average, certain environmental properties affect SOC and SOC stock [Rodríguez-Lado and Martínez-Cortizas, 2015]. However, they are bounded by definition to model the conditional mean, thus being unable to explore the effects of the same properties at different C contents or stock of the soil, especially at the boundaries of the distribution.

In the present work, Quantile Regression (hereafter QR, [Koenker \[2005\]](#)) is used to model SOC stock from a non-homogenously sampled topsoil SOC dataset using soil texture, land use, topographic and remotely sensed covariates. In particular, QR is able to model the relationship between a set of covariates and specific percentiles of SOC. In classical regression approaches, the regression coefficients (also often called beta coefficients) represent the mean increase in the response variable produced by one unit increase in the associated covariates. Conversely, the beta coefficients obtained from QR represent the change in a specific quantile of the response variable produced by a one unit increase in the associated covariates. In this way, QR allows one to study how certain covariates affect, for example SOC median (quantile $\tau = 0.5$) or extremely low (e.g., $\tau = 0.05$) or high (e.g., $\tau = 0.95$) SOC values. Therefore, it gives a much more complete description of the effect of predictors on the whole SOC probability distribution (i.e., not just the mean) and thus offer the chance to study differential SOC responses to environmental factors.

Furthermore, when used for mapping purposes, QR also allows for soil mapping at given quantiles, providing analogous estimates to more common approaches by using the median instead of the mean.

In the present experiment we use a nested strategy to model SOC in Sicilian agricultural areas with QR: we initially aim at testing the QR overall performances when modeling the SOC stock by segmenting its distribution into 19 quantiles ($\tau = 0.05$ to $\tau = 0.95$). Subsequently, we examine the coefficients of each predictor for each of the quantiles. Ultimately, we compare the median prediction with available SOC benchmarks for the same study area to test the efficiency of QR for soil mapping purposes. The dataset used in this contribution is the same used in [Schillaci et al. \[2017b\]](#) where a Stochastic Gradient Treeboost is adopted.

2 Materials and methods

2.1 Study area

Sicily with its approximate 25 thousand squared kilometers is the biggest Mediterranean island. More than 60% of its area is cropped. The natural/semi natural ecosystems include i) Mediterranean maquis, ii) dunes and coastal systems, iii) woods and forests. There are also 37 ancillary islands that are not considered in the present study. Sicily has several sub-climatic zones, all of which are included in hot-summer Mediterranean climate (Csa Koeppen) and warm-summer Mediterranean climate (Csb Koeppen) with mean annual temperatures usually higher than 15.8° C. From the West to the South-East coasts, indicators of a semiarid environment can be observed over the year with low or no rainfall summer, high air temperatures and evapo-transpiration demand together with water deficit. The mountainous areas (Madonie, Sicani, Nebrodi and Peloritani ridges, physiography can be checked in [Schillaci et al. \[2017a\]](#)) are scarcely cultivated mostly because of conservation policies acting in favor of the local temperate woodland. The continentality index, which is determined by the difference between the mean air temperature during summer and winter, is similar in all the climatic subregions.

According to the latest soil map published by [Fantappiè et al. \[2010\]](#) using the World Reference Based [\[Group et al., 2014\]](#) soil classification, the dominant soils in Sicily are:

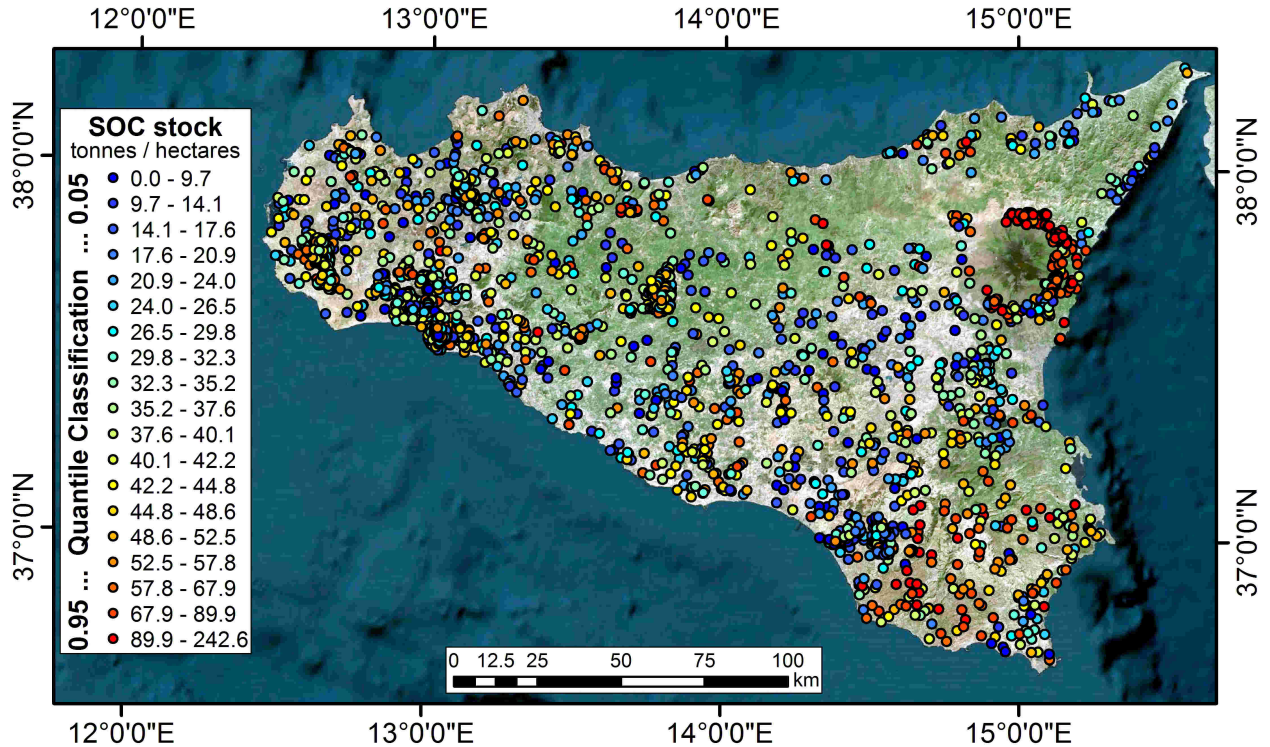


Figure 1: SOC stock dataset and geographic contextualization.

Entisols (36%), Inceptisols (34%), followed by the Mollisols, Alfisols, Vertisols and Andisols. This climatic context plays an important role on the decay processes of organic residue [Lützwow et al., 2006] and on the stabilization of organic fractions. In particular, the local climatic setting facilitates the decomposition and mineralization of the organic matter.

2.2 SOC Data

The available datasets represent the SOC stock (expressed in $ton \cdot ha^{-1}$) of the topsoils (Ap horizon, from 0 to 30cm depth) primarily from agricultural areas (Figure 1). It has been calculated from the organic carbon (expressed in $g \cdot kg^{-1}$) multiplied by the soil bulk density. The latter is derived by pedotransfer function [Pellegrini et al., 2007]. In total, 2202 samples are used for modeling purposes. See [Schillaci et al., 2017b] for further information on the dataset.

Supplementary Figure 1 shows the variability associated with each of the considered quantiles. The dataset was provided by the Assessorato Regionale Territorio Ambiente (ARTA) as georeferenced SOC values derived by pedological profiles.

The adopted covariates and their interpretation are discussed in the Supplementary Materials, Predictors Section. The distribution of the aforementioned covariates is shown in Supplementary Figure 2 through their Empirical Cumulative Distribution Function. Prior to any analysis, we transformed some of the variables. This is shown and explained in the Supplementary Material (Figure 3 and Pre-processing Section, respectively).

2.3 Statistical modeling using quantile regression

2.3.1 Quantile regression

In classical regression analysis, the fluctuations in the mean of a response variable (e.g., $\log(\text{SOC})$) are typically explained through a linear function of a set of predictors. In the case where n responses Y_1, \dots, Y_n are observed with their p respective predictors x_{1i}, \dots, x_{pi} (here assumed to be continuous for simplicity), a statistical model may be formulated as

$$Y_i = \beta_0 + \beta_1 x_{1i} + \dots + \beta_p x_{pi} + \varepsilon_i,$$

where the random variables ε_i are typically assumed to be mutually independent and to follow a normal distribution with zero mean and finite variance σ^2 . Under such a model, and if the predictors are linearly independent, the vector of unknown regression parameters $\beta = (\beta_1, \dots, \beta_p)^T$ may be estimated using the Ordinary Least Squares (OLS) estimator $\hat{\beta}_{(OLS)}$, which may also be seen as minimizing the squared loss function, i.e.,

$$\hat{\beta}_{OLS} = (X^T X)^{-1} X^T Y = \min_{\beta} \|Y - X\beta\|^2 = \min_{\beta} \sum_{i=1}^n (Y_i - \beta_0 - \beta_1 x_{1i} - \dots - \beta_p x_{pi})^2, \quad (1)$$

where $Y = (Y_1, \dots, Y_n)^T$ is the vector of observations, and X is the n -by- $(p+1)$ design matrix, where the first column corresponds to the intercept and is a vector of ones, and each other column corresponds to a specific predictor, i.e., it contains the values x_{k1}, \dots, x_{kn} , $k = 1, \dots, p$. From the right-hand side of (1), the conditional *mean* of Y may be estimated by $\hat{\beta}_{0;OLS} + \hat{\beta}_{1;OLS}x_1 + \dots + \hat{\beta}_{p;OLS}x_p$. In other words, this is a *point predictor*, focusing on a single feature (i.e., the mean) of the distribution of the response Y .

More detailed information on the whole conditional (not necessarily Gaussian) *distribution* of the response Y may be obtained using *quantile* regression. By definition, for each probability $0 \leq \tau \leq 1$, the τ -quantile y_{τ} of Y is the value exceeding $(100 \times \tau)\%$ of the data. Mathematically, one has $\text{pr}(Y \leq y_{\tau}) = \tau$, and the collection of all quantiles $\{y_{\tau} : 0 \leq \tau \leq 1\}$ fully characterizes the probability distribution of Y . The value $\tau = 0.5$ corresponds to the *median*, while low and high quantiles (for low and high values of τ , respectively) correspond to extreme values of Y lying in the lower and upper tails of the distribution, respectively.

By analogy with (1), the conditional τ -quantile may be estimated by minimizing an objective function, where the squared loss function is replaced by the quantile loss function. More precisely, computing

$$\hat{\beta}_{\tau} = \min_{\beta} \sum_{i=1}^n L_{\tau}(Y_i - \beta_0 - \beta_1 x_{1i} - \dots - \beta_p x_{pi}), \quad (2)$$

where the quantile loss function L_{τ} is defined as

$$L_{\tau}(x) = \begin{cases} -2(1 - \tau)x, & x < 0; \\ 2\tau x, & x \geq 0, \end{cases}$$

the conditional τ -quantile y_{τ} may then be estimated as $\hat{y}_{\tau} = \hat{\beta}_{0;\tau} + \hat{\beta}_{1;\tau}x_1 + \dots + \hat{\beta}_{p;\tau}x_p$. When $\tau = 0.5$, $L_{0.5} = |x|$ is the absolute loss function, and $\hat{y}_{0.5}$ corresponds to the estimated

conditional median. In our application, we choose a sequence of 19 equispaced probabilities $\tau = 0.05, 0.1, \dots, 0.95$ to fit separate quantile regression models, giving much deeper insight into the complete conditional distribution of the SOC values, as a function of spatial predictors. By focusing on low (respectively high) quantiles, regression coefficients inform us about the predictors mostly influencing the absence (respectively high concentrations) of SOC stock over space. By considering independent quantile regression models for different values of τ , this allows for the possibility that the importance of certain predictors may change according the SOC level. More statistical details on quantile regression and its application may be found in [Koenker \[2005\]](#).

Finding the estimated parameters $\hat{\beta}_\tau$ by optimizing (2) is not trivial, but robust algorithms have been implemented and made freely available in the R package `quantreg`. Model checking and validation may be performed using classical regression techniques with some minor adjustments. For example, to assess the goodness of fit, the coefficient of determination R^2 is typically replaced by a similar measure based on the quantile loss, although the interpretation remains essentially the same. Similarly, to check the ability of the model to predict unobserved values, cross-validation combined with the quantile loss function is typically used, in order to be consistent with the fitting procedure, instead of using the mean squared error as in classical regression analysis.

2.3.2 Model building strategy, estimation and uncertainty assessment

The strategy adopted in the present work includes five steps:

1. We perform a preliminary multicollinearity analysis to exclude highly correlated covariates. When Pearson’s correlation coefficients are above 0.7 or below -0.7, we remove one of two or more collinear covariates as suggested by [\[Pengelly and Maass, 2001\]](#). This is shown and explained in the Supplementary Material (Figure 4 and Pre-processing Section, respectively).
2. Categorical covariates are converted into dummy variables equivalent to each predictor level. Then, the most and least representative dummy classes are removed to avoid using a singular design matrix and subsequent parameter estimates. The least represented classes contain one to five SOC stock samples. This allows to remove potential sources of noise in the modeling procedure, whereas the effect of the most frequent class are carried in the model intercept. The most frequent classes account for a significant part of the data by definition, thus the interpretation of their contribution to the model is clearly important. To investigate their effects on SOC stock we pre-run a separate simpler model built only with the most frequent class within the covariates.
3. Model performances or predictive power is evaluated through leave-one-out cross-validation [\[Sammut and Webb, 2010\]](#). This allows for producing quality metrics based on quantile loss [\[Koenker and Bassett Jr, 1978\]](#). In a QR framework, the latter is equivalent to the R^2 coefficient used in classical linear regression.
4. Model uncertainty over replicates is implemented through non-parametric case-resampling bootstrap [\[Davison and Hinkley, 1997\]](#). In particular, 10000 replicates are generated

by resampling each of the 2202 cases with replacement. As a result, 10000 replicates of the beta coefficient estimates for each predictor and categorical class are produced for each of the 19 quantiles considered in this study. Similarly, 19 sets of 10000 predictive maps are also computed. This procedure evaluates the variability of the modeling output and the reliability of the final estimates across replicates.

5. SOC regionalization is conducted by producing 19 distinct quantile predictive maps by using the original dataset without any resampling scheme to ensure the full predictive power for mapping purposes.

2.4 Currently available SOC estimations in the study area

Three digital soil mapping products are currently available for the area under study: i) the ISRIC World Soil Information (<http://www.isric.org>, Hengl et al. [2014]), ii) the Global Soil Organic Carbon Estimates of the Harmonized World Soil Database (<http://esdac.jrc.ec.europa.eu/content/global-soil-organic-carbon-estimates>, Hiederer and Köchy [2011]) and iii) the European Joint Research Centre JRC European SOC map [Lugato et al., 2014]. These layers represent the state of the art of digital soil mapping and are de facto the only SOC benchmarks for the globe and for Europe. According to Hengl et al. [2014], SOC distribution is calculated through Generalized Linear Models at a 1-km resolution using the GSIF package in R. Hiederer and Köchy [2011] use analogous linear regression model and spatial resolution to regionalize the SOC data over the globe. Conversely, the JRC European estimates are calculated using a deterministic approach using the agro-ecosystem SOC model CENTURY [Parton et al., 1988]. The inclusion of such estimates in the present contribution allows to compare the regional QR prediction to reliable, robust and well tested analogous datasets. The comparison is based on the median QR prediction together with the aforementioned benchmarks. To accommodate for differences in the spatial resolution we downscale all maps to the minimum common resolution (1-km cell size) where the resulting values per pixel represent the average SOC stock among smaller pixels in a given 1-km cell side.

3 Results

Leave-one-out cross-validation performances appear in line with other methods in the literature. In particular, Schillaci et al. [2017b] report an R^2 of 0.47 whereas the quantile loss reaches 0.49 for quantiles $\tau = 0.4, 0.45$ (see Figure 2). In addition, Figure 2 reveals that the quantile loss has a bell shape as a function of the quantile level. This implies that the predictive power decreases towards the boundaries of the distribution.

The uncertainty of estimated beta coefficients (assessed by means of the non-parametric case-resampling bootstrap) is presented in five separate subplots: Figure 3 presents boxplots of estimated parameters obtained from the 10000 bootstrap replicates for the simple model comprising only three categorical variables; The estimated parameters for the final reference model are summarized in Figures 4, 5, 6, and 7, which correspond to continuous predictors, Land use, Texture and Landform, respectively.

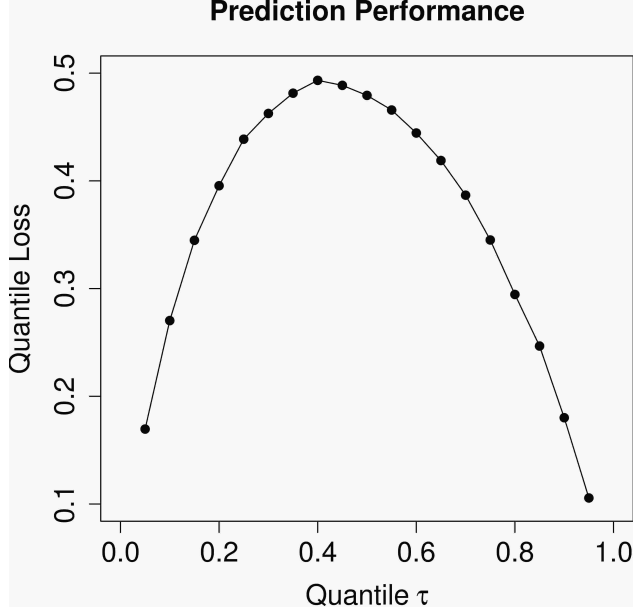


Figure 2: Leave-one-out performance evaluation through quantile loss.

The spatial prediction and its uncertainty are summarized in Figures 8, 9 and 10.

The simple model (see Figure 3) accounts for the most represented categorical classes in Land use (*Non-irrigated arables*), Texture (*Clay loam*) and Landforms (*Plains*). This model is characterized by a very low variability of the intercept. *Non-irrigated arables* and *Clay loam* are negatively associated with SOC, and beta coefficients show a tendency to further decrease at the upper quantiles, especially for the textural class. *Plains* scarcely influences the SOC stock.

For the final model, some covariates clearly appear dominant, this being shown through high deviations from the blue line corresponding to zero beta coefficient along the quantiles. This particularly occurs for the continuous the covariates $\log(\text{Catchment Area})$, *Mean Annual Rainfall* and *Mean Annual Temperature* as shown in Figure 4. *Mean Annual Temperature* shows a negative trend at quantiles < 0.15 . Conversely, $\log(\text{Catchment Area})$ and *Mean Annual Rainfall* contributions to the prediction are always positive. Other predictors including *Northness*, *Eastness* contribute to SOC stock increase whereas *Slope* reduces it.

The effects of *Land Use* are reported in Figure 5 where *Vineyards* and *Olive orchards* (Corine Code 221 and 223, respectively) show a positive relationship with organic carbon content and a tendency for beta coefficients to decrease towards the upper quantiles. Conversely, coefficients of *Land principally occupied by agriculture, with significant areas of natural vegetation*, *Natural grassland* and *Sclerophyllous vegetation* are slightly but constantly positive.

The analogous representation for *Texture* is shown in Figure 6. Here, the role of Texture emerges for few textural classes. In particular, *Silty Loam*, *Silty Clay Loam*, and *Sandy* textures appear to be strongly, mildly, and weakly positive, respectively, even across all quantiles. The mean beta coefficient per quantile in *Clay* and *Sand* shows an opposite pattern. On the one side, clay texture yields very high positive beta coefficients at lower quantiles and decreases approximately to zero to the right tail of the SOC distribution. A

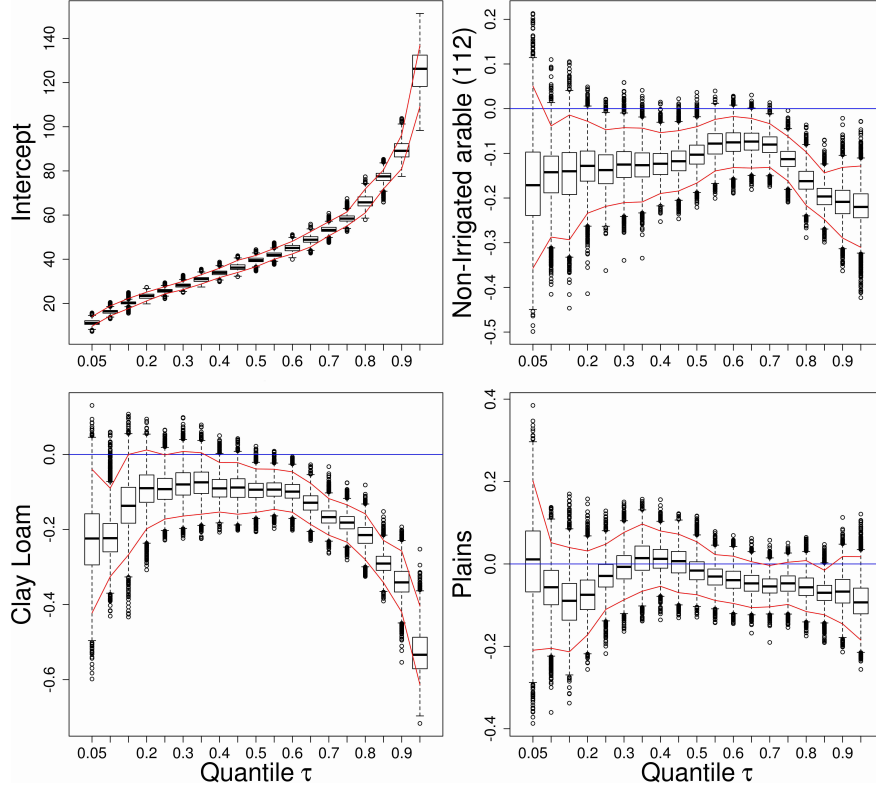


Figure 3: Boxplots of estimated beta coefficients based on the simple model with 10000 bootstrap replicates, and plotted with respect to the quantile level $\tau = 0.05, \dots, 0.95$. The blue line represents 0 (i.e., no effect), while the red curves are 95% pointwise confidence intervals.

similar, but less pronounced decrease in the beta coefficients is shown for the *Silty Clay*. Both *Clay* and *Silty clay* present a very low internal variability, especially at the upper quantiles. On the other side, sand texture class produces an increasing beta coefficient across the quantiles, from strongly negative to the left side of the distribution to almost 0 in the right side. However, the variability within each beta coefficient in each quantile for sand is very high, hindering its interpretation.

Coefficients for *Landform* classes are summarized in Figure 7 (except for *Plains*) where unexpectedly, none of the Landform classes appear to have a clear influence over the SOC in the study area and no pattern across quantiles can be ascertained.

Predictive maps are shown in Figure 8. Here, variations in predicted SOC over the study area are evident in the extreme quantiles ($q \leq 0.25$ and $q \geq 0.75$) but less pronounced in the central quantiles ($0.25 < q < 0.75$). Similarly, the variability (measured as inter-quantile range) shows an increasing trend through quantiles.

The qualitative comparison between the predicted median and those of ISRIC, European and Global JRC benchmarks is shown in Figure 9. Among the available SOC Stock benchmarks, the JRC European map and, to a certain degree, ISRIC map are close to our median map in term of degrees of spatial variability (Figure 10). ISRIC frequently overesti-

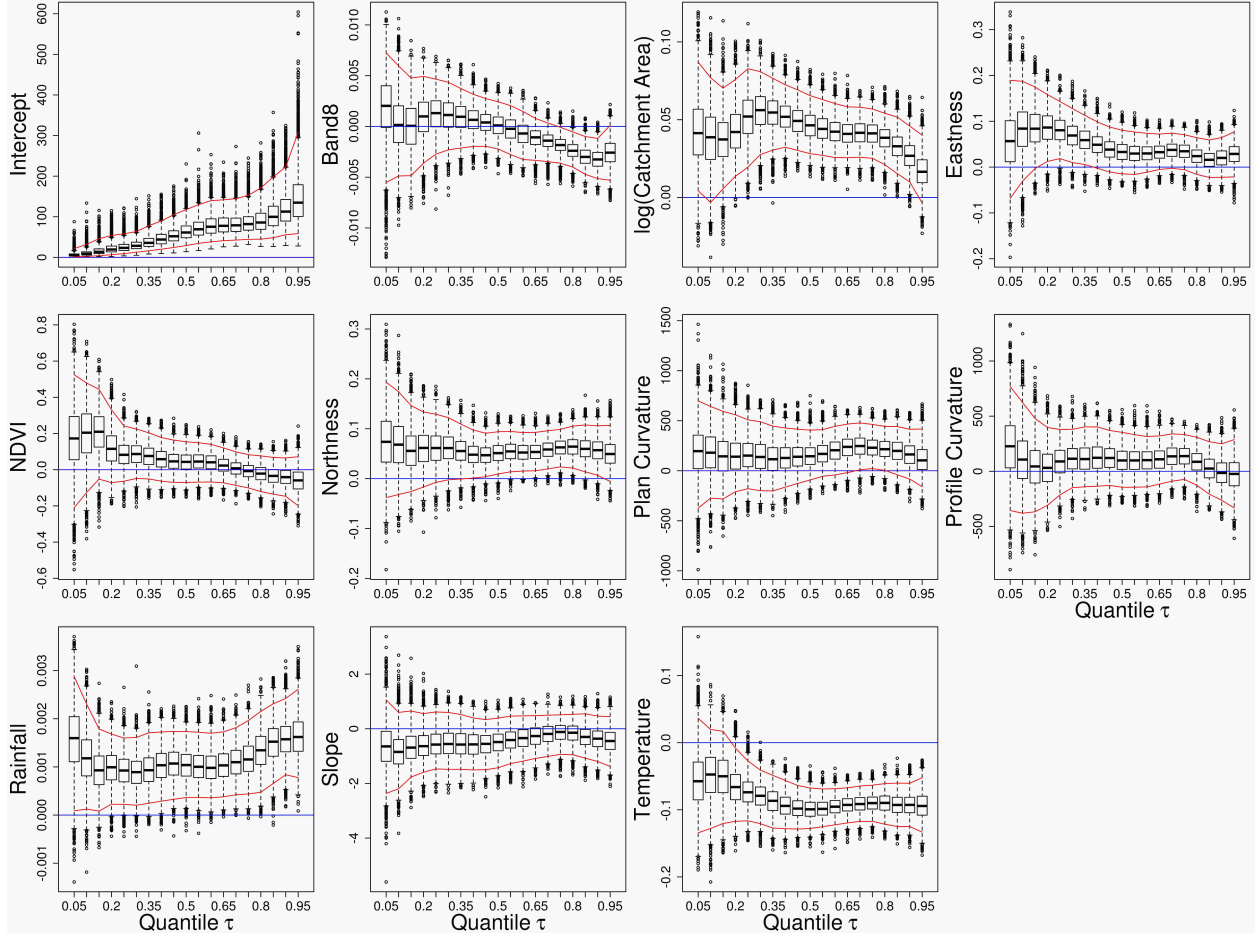


Figure 4: Boxplots of estimated beta coefficients for continuous predictors. These results are based on the final model with 10000 bootstrap replicates, and plotted with respect to the quantile level $\tau = 0.05, \dots, 0.95$. The blue line represents 0 (i.e., no effect), while the red curves are 95% pointwise confidence intervals.

mates SOC stock in the study region. In particular, our predicted median and ISRIC maps efficiently capture the pedo-genetic differences but not differences within land use classes. JRC-EU better capture differences within arables, which was far the most represented classes of land use. Finally, JRC-GL captures few spatial differences but, similarly to our predicted median it is the only benchmark capturing the high SOC stocks in the southeastern areas.

The spatial relation between predictive maps is compressed for a numerical-only assessment in Figure 10.

Here, the reference predicted median is compared to the three benchmarks through i) pixel-by-pixel density plotting, ii) quantile-quantile plot, iii) residuals. Three observations can be made. ISRIC is strongly overestimating the SOC stock compared to our QR-based model only with low-carbon coincident concentrations. The qualitative similarity between the median and the JRC-EU predictions is once more confirmed from a quantitative perspective with a quantile-quantile plot showing a slight but constant underestimation. Ultimately,

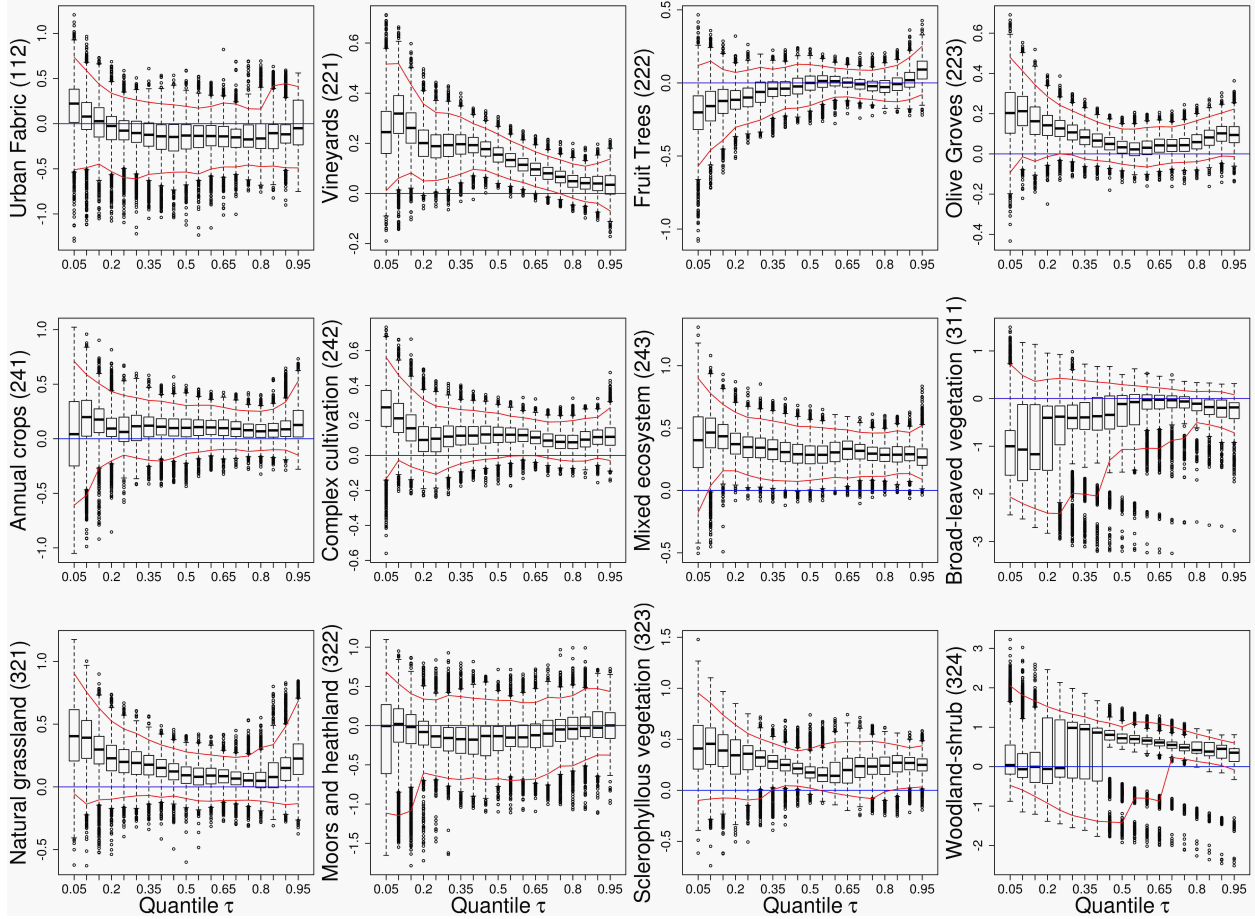


Figure 5: Boxplots of estimated beta coefficients for each category of Land Use. These results are based on the final model with 10000 bootstrap replicates, and plotted with respect to the quantile level $\tau = 0.05, \dots, 0.95$. The blue line represents 0 (i.e., no effect), while the red curves are 95% pointwise confidence intervals. Numbers between parentheses correspond to the Corine 2000 codes. In particular, Mixed ecosystem corresponds to Land principally occupied by agriculture, with significant areas of natural vegetation (Corine 243).

JRC-GL shows the lowest residuals with respect to the QR reference together with a good agreement up to a concentration of approximately 45 t/ha . However, from this threshold to the right tail of the distribution, the two predictions completely diverge one from the other.

4 Discussion

We present a Quantile Regression framework for modeling SOC stock data. This is applied to the semi-arid Sicilian territory located in the middle of Mediterranean Sea. We explore its application evaluating its predictive performances and assess it as a tool to provide a deeper information on predictor effects at different carbon contents. This makes QR a tool to produce reliable soil maps.

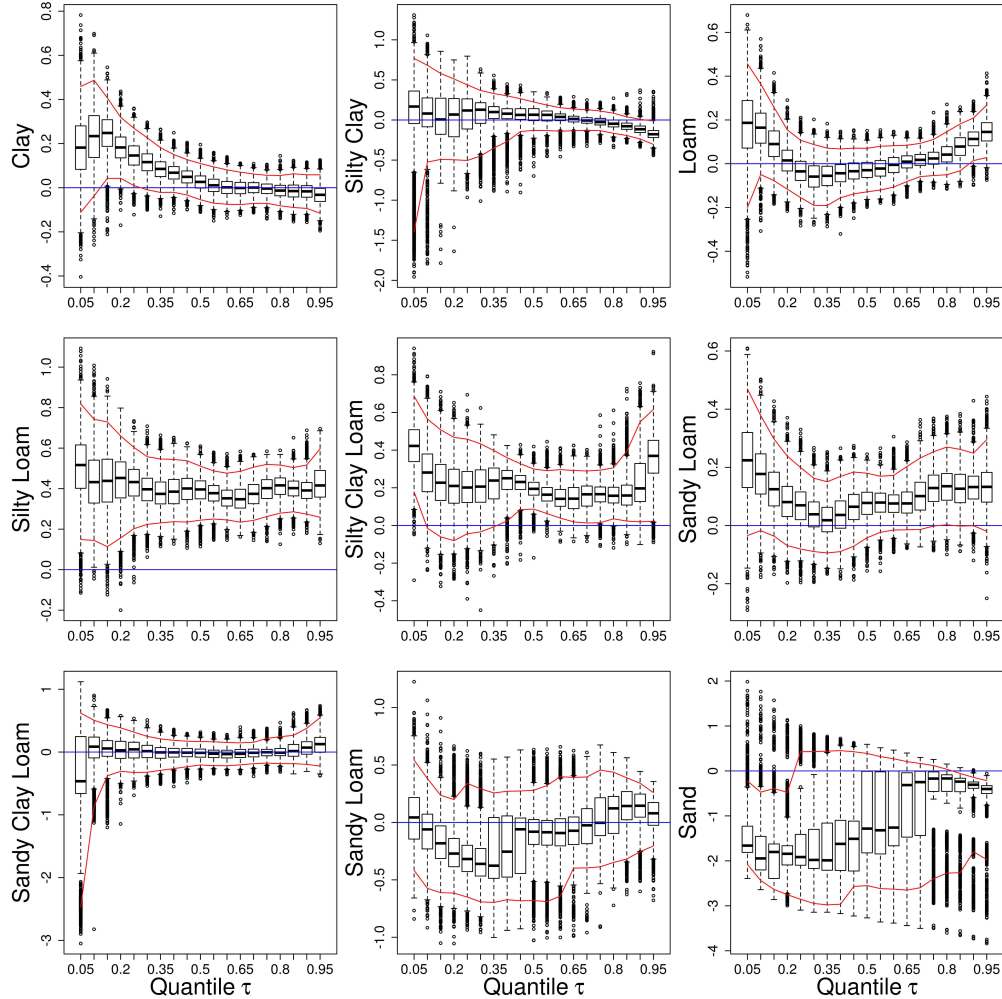


Figure 6: Boxplots of estimated beta coefficients for each category of Texture. These results are based on the final model with 10000 bootstrap replicates, and plotted with respect to the quantile level $\tau = 0.05, \dots, 0.95$. The blue line represents 0 (i.e., no effect), while the red curves are 95% pointwise confidence intervals.

In terms of predictive skills, QR shows comparable results (maximum R^2 of 0.49, in Figure 2) to those obtained with Stochastic Gradient Treeboost (R^2 of 0.47, Schillaci et al. [2017b]) using the same dataset.

Other experiments show equivalent or worse performances. Yigini and Panagos [2016] obtain an R^2 coefficient of 0.40 at the European scale with regression-kriging, whereas Meersmans et al. [2008] report an R^2 coefficient of 0.36 with multiple regression and Nussbaum et al. [2014] R^2 of 0.35, both at regional scales. Quality metric based on the quantile loss highlights a decreased performance near the left and right tails of the SOC stock distribution.

The simple model intercept (Figure 3) shows values bounded between 10 and 130 t/ha which are in line with the original dataset and interestingly these values show a very low variability. This implies that the contribution of *Non-irrigated arables*, *Clay loam*, and, to a lesser extent, *Plains* is very strong. Notably, the intercept of the final model (Figures 4),

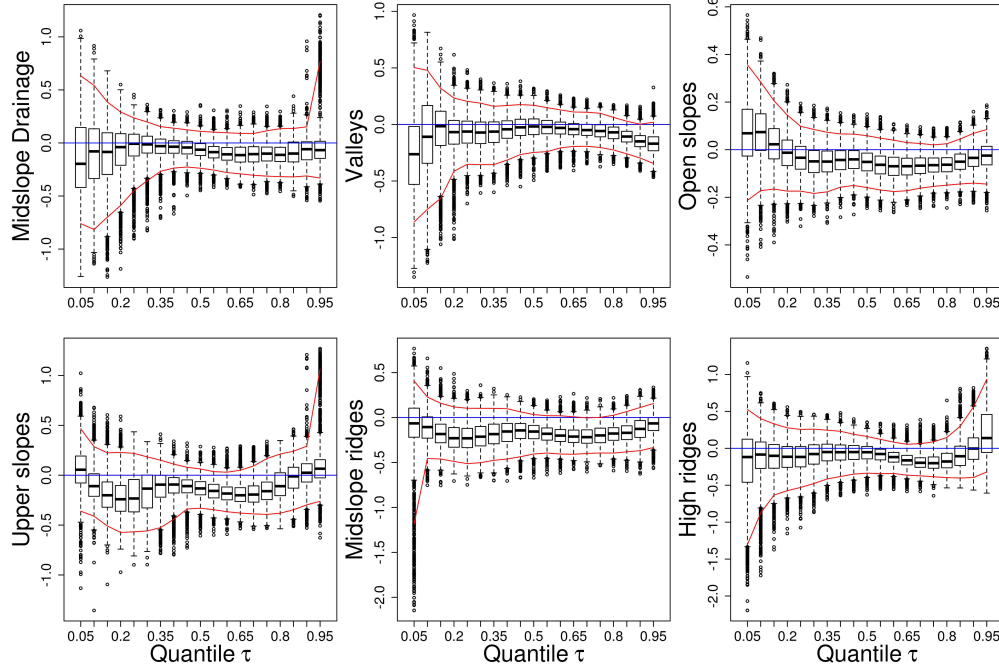


Figure 7: Boxplots of estimated beta coefficients for each category of Landform Classification. These results are based on the final model with 10000 bootstrap replicates, and plotted with respect to the quantile level $\tau = 0.05, \dots, 0.95$. The blue line represents 0 (i.e., no effect), while the red curves are 95% pointwise confidence intervals.

that also bears the effects of the *Non-irrigated arables*, *Clay loam* and *Plains*, shows values very similar to the simple model but a higher variability. This implies that the greater model complexity due to the inclusion of other predictors (both for continuous and categorical) can produce high ranges of variation in the SOC stock.

Mean Annual Rainfall and $\log(\text{Catchment Area})$ coefficients are constantly positive, confirming the influence of soil moisture on carbon sequestration as reported in several articles [e.g., Saiz et al., 2012]. Nonetheless, these result partly disagree with Schillaci et al. [2017b], that found that found a scarce, but still positive, influence of the untransformed CA on SOC stock of the same area, with a method capable of handling non-gaussian distributed data. This difference points at the need of transforming data even for non-strictly statistical predictive methods.

In contrast to *Mean Annual Rainfall* and $\log(\text{Catchment Area})$, *Mean Annual Temperature* shows negative and slightly varying beta coefficients across the whole SOC distribution. Recent surveys clearly highlight the balance between temperature and rainfall in shaping the background SOC and SOC stocks amount and variations ([Davidson et al., 2000, FAO, 2017, Schillaci et al., 2017a]).

However, the community still debates whether the temperature should have a positive correlation with SOC stocks [e.g., Conant et al., 2011, Sierra et al., 2015]. In the present work, the strong and negative effect of the temperature supports the hypothesis that temperature negatively affects SOC accumulation in agricultural soils of Mediterranean areas even when

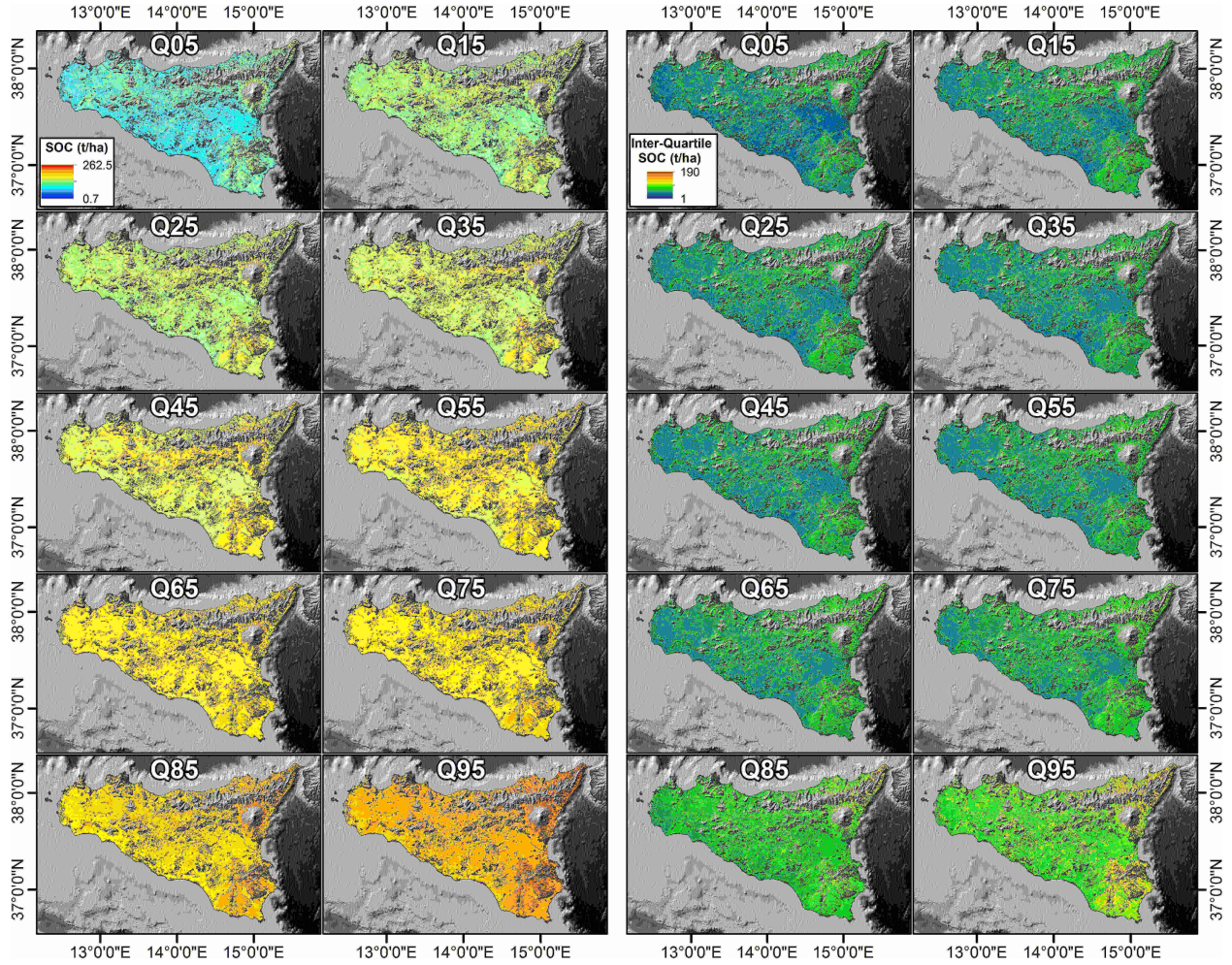


Figure 8: Predictive maps (left side) together with their associated variability (right side). The latter is measured as the interquartile range, i.e., the distance between the 75% and the 25% quantiles, calculated from the 10000 cross-validated maps. Greyed out regions correspond to no-data zones.

SOC or rainfall or both are high. This could depend on the erraticness of rainfall and thus water availability that can consist in a low water availability even at high rainfall, which can be lost by runoff [Panagos et al., 2017]. The unclear but apparently low temperature effect and clear and positive rainfall effect at the lowest quantiles also suggests that when SOC is low, management of water availability rather than temperature mitigation should be put in place.

Ultimately, SL beta coefficients across quantiles are almost constantly negative confirming the influence of erosion on carbon stocks [Olson et al., 2016].

From textural classes a general positive trend for mixed granulometries emerges. This is typical for Sicilian soils as sand classes do not have the capacity to fix organic matter while purely clayey soils are extremely variable. A peculiar effect actually characterizes the Clay class with a positive beta coefficient sign from quantile 0.05 to 0.50 aligning to zero values from the median to the 95 percentile. This can be interpreted as a strong clay protective

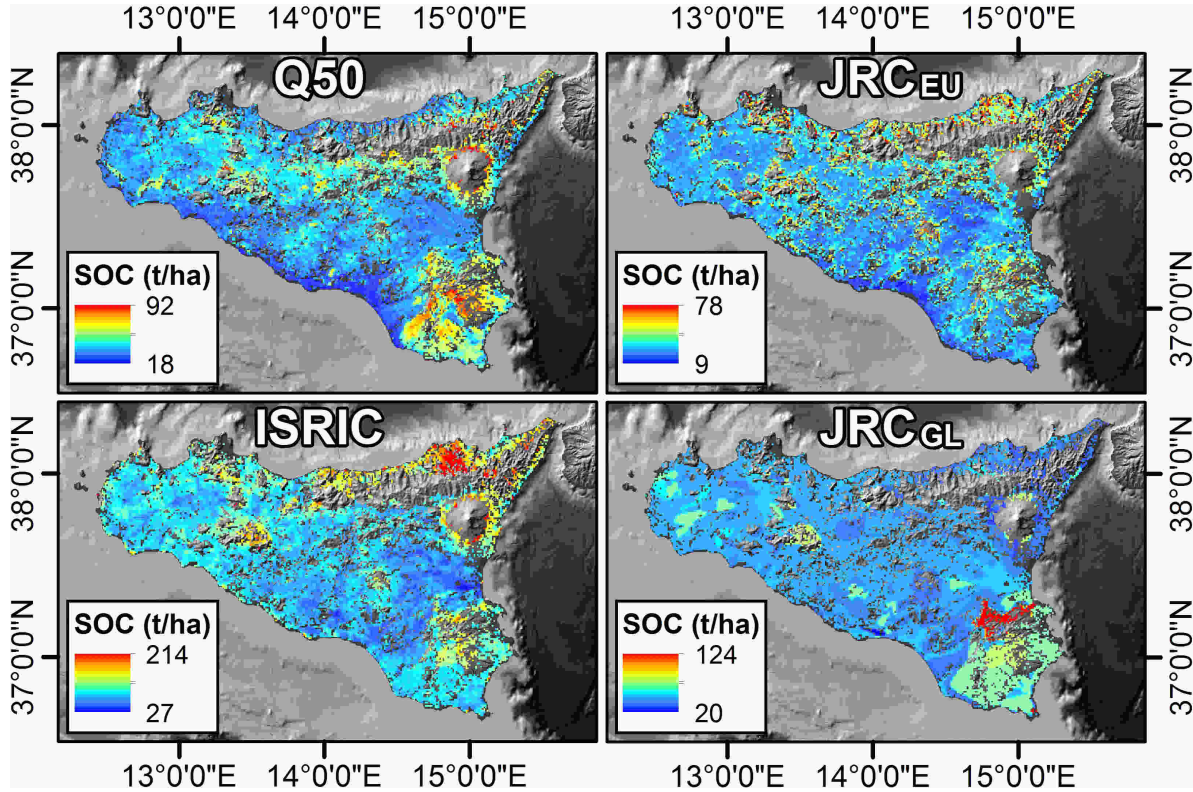


Figure 9: Available SOC-stock spatial-predictive maps in Sicily: Q50 corresponds to our median prediction, ISRIC is the SOC stock map from the International Soil Reference and Information Centre whereas JRC-EU and JRC-GL are the SOC stock benchmarks produced from the Joint Research Centre at the European and Global scale, respectively. Greyed out regions correspond to no-data zones.

effect for small carbon contents up to a limit where other factors need to interplay in order to further increase the carbon fixation/absorption [Badagliacca et al., 2017, Grimm et al., 2008, Mondal et al., 2016].

Among different uses strong positive relations can be recognized for *Vineyards, Olive Groves, Land principally occupied by agriculture, with significant areas of natural vegetation, Natural Grassland and Sclerophyllous vegetation*. [Vicente-Vicente et al., 2016] report carbon sequestration rates of $0.78 \text{ tC ha}^{-1} \text{ yr}^{-1}$ Mediterranean vineyards. Similarly, Farina et al. [2017] suggest a potential SOC stock increase of 40.2% and 13.5% for vines and olives in similar environments to those considered in this study, respectively. In our work, such a positive effect were found also at the lowest boundary of the SOC distribution. This has a direct implication for land use management when aiming to increase SOC in such a fragile ecosystems compared to arables. In Sicily, arables are mostly winter cereals and grain legumes, which respectively reduce N availability for the microorganisms and have few residues.

Similarly, the positive effects of *Land principally occupied by agriculture, with significant areas of natural vegetation (Corine 243)* suggest that in-field and in-farm crop and landscape and environmental diversification can also favor SOC accumulation irrespective of the initial

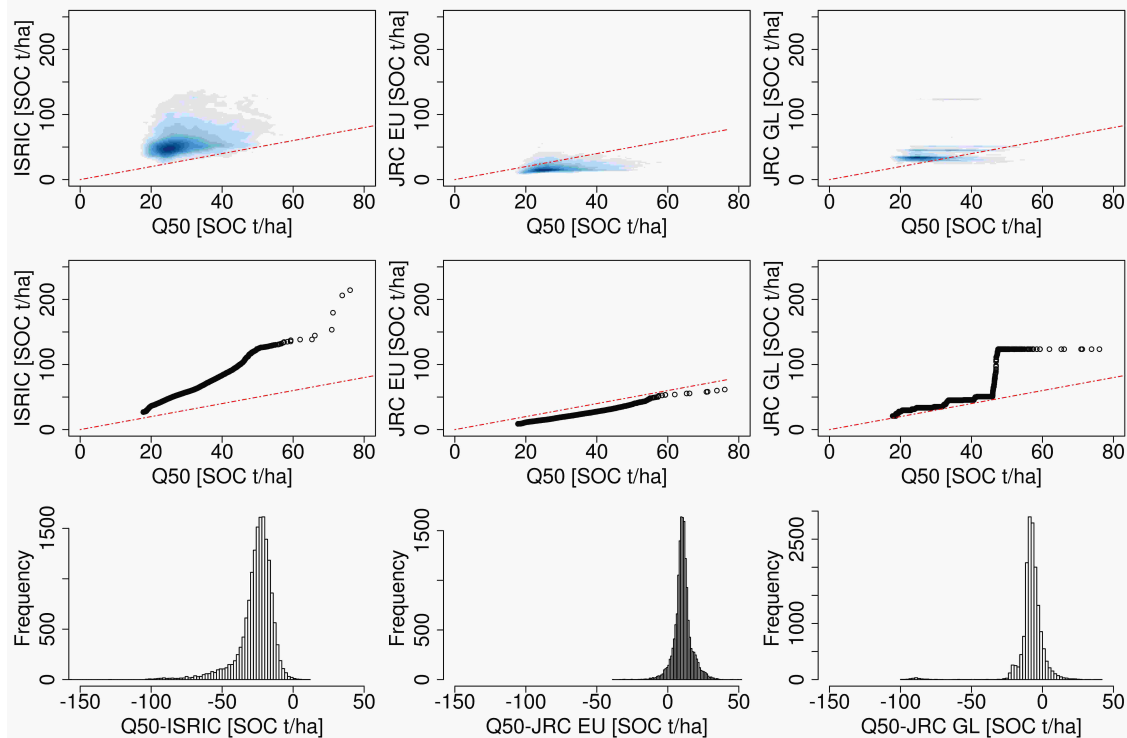


Figure 10: Bivariate comparison between median and available benchmark. The first row shows a density scatterplot between our predicted median map and the three available benchmarks in each column. The second row presents the same information compressed in a quantile-quantile plot. The third row summarises the residuals. Red dashed lines correspond to linear fits with regression coefficients equal to 1.

SOC levels in semi-arid Mediterranean environments, as also found in continental north-European areas by [Kaczynski et al. \[2017\]](#). Their work cover the time window between 1971 and 2013 during which the authors highlight a marked increase in SOC stock from 2001 coinciding with crop production as a very high yields provided very high input of carbon from crop residues. With respect to *Land principally occupied by agriculture, with significant areas of natural vegetation*, [Tian et al. \[2016\]](#) conduct a study in China in order to estimate carbon sequestration in different grassland quality condition, which also depend on the diversification of its composition. Their conclusions show that the average sequestration rate was $0.04 \cdot 10^{12} \text{ kgC} \cdot \text{ha}^{-1}$ and that this rate increases as the grassland quality increases, which also depends on the diversification of its composition.

As regards the Sclerophyllous vegetation, other studies have highlighted its contribution to SOC even in Mediterranean contexts [[Muñoz-Rojas et al., 2013](#)].

In terms of soil mapping, the four maps (our median and the three benchmarks) agree in depicting higher SOC stock levels around the Etna volcano and generally at the foothills. This may be interpreted as a result of particle transport where Carbon-rich soil from reliefs are eroded and deposited at the bottom of mountain ranges and/or different geological substrates producing soils with contrasting ability to retain organic C [[Costantini and L'Abate, 2016](#), [Mondal et al., 2016](#)]. A similar agreement is produced in the central portion of the

study area but with lower SOC concentrations. Conversely, the southeastern sector is shown to carry high SOC stocks for three maps with the exception of the European JRC, whereas the Global JRC depicts less reasonable patterns and ISRIC overestimates the SOC stock with peaks well above any local measurement. Our SOC stock predictive map shows reasonable values such as JRC and reasonable spatial patterns such as ISRIC. This can clearly be due to a higher resolution because ISRIC, Global and European JRC are continental or global and at such scale the landscape scale is often not represented. Nevertheless, QR was able to reach this level of detail suggesting its use for different datasets and modeling scales.

5 Conclusion

QR performs similarly to other statistical methods and enables considerations at given sub-domains of the SOC stock distribution. The link between SOC stock amount and the distribution of some Land Use classes (Vineyards, Olive orchards and Mixed ecosystems (Corine 243)) or and presence of Clayey soils was positive and, above all, varying across the SOC distribution. This has direct implication in the management of agriculture at the regional level, since these crops are likely to contemporary increase the gross income of the area and also the ecosystem benefits, such as C sequestration in the soil.

Variables like Vineyards or Clay change significantly through the SOC distribution. This suggest that classical linear regression methods may not recognize this trend and ultimately generate very different SOC values at high or low carbon contents. Furthermore, advantages can be drawn from an agronomic point of view as a better understanding of environmental effects at various SOC concentrations can improve management schemes and allow for sequestration-tailored practices that preserve yield and rentability. This paper shows that Quantile Regression has valid and interesting agronomic applications, as observed in few recent examples [Barnwal and Kotani, 2013, Yu et al., 2016]. To promote its applicability and reproducibility, the R code is made available in the Supplementary Materials.

References

- Mohammad Ajami, Ahmad Heidari, Farhad Khormali, Manouchehr Gorji, and Shamsollah Ayoubi. Environmental factors controlling soil organic carbon storage in loess soils of a subhumid region, northern iran. *Geoderma*, 281:1–10, 2016.
- Stephen IC Akpa, Inakwu OA Odeh, Thomas FA Bishop, Alfred E Hartemink, and Ishaku Y Amapu. Total soil organic carbon and carbon sequestration potential in nigeria. *Geoderma*, 271:202–215, 2016.
- Jane Kelly Silva Araujo, Valdomiro Severino de Souza Júnior, Flávio Adriano Marques, Paul Voroney, and Regilene Angelica da Silva Souza. Assessment of carbon storage under rainforests in humic hapludox along a climosequence extending from the atlantic coast to the highlands of northeastern brazil. *Science of The Total Environment*, 568:339–349, 2016.

- Giuseppe Badagliacca, Paolo Ruisi, Robert M. Rees, and Sergio Saia. An assessment of factors controlling n₂o and co₂ emissions from crop residues using different measurement approaches. *Biology and Fertility of Soils*, 2017.
- Prabhat Barnwal and Koji Kotani. Climatic impacts across agricultural crop yield distributions: An application of quantile regression on rice crops in andhra pradesh, india. *Ecological Economics*, 87:95–109, 2013.
- Long-Fei Chen, Zhi-Bin He, Xi Zhu, Jun Du, Jun-Jun Yang, and Jing Li. Impacts of afforestation on plant diversity, soil properties, and soil organic carbon storage in a semi-arid grassland of northwestern china. *Catena*, 147:300–307, 2016.
- Richard T Conant, Michael G Ryan, Göran I Ågren, Hannah E Birge, Eric A Davidson, Peter E Eliasson, Sarah E Evans, Serita D Frey, Christian P Giardina, Francesca M Hopkins, et al. Temperature and soil organic matter decomposition rates—synthesis of current knowledge and a way forward. *Global Change Biology*, 17(11):3392–3404, 2011.
- Edoardo A.C. Costantini and Giovanni L’Abate. Beyond the concept of dominant soil: Preserving pedodiversity in upscaling soil maps. *Geoderma*, 271:243–253, 2016. ISSN 0016-7061. doi: 10.1016/j.geoderma.2015.11.024.
- Fuqiang Dai, Qigang Zhou, Zhiqiang Lv, Xuemei Wang, and Gangcai Liu. Spatial prediction of soil organic matter content integrating artificial neural network and ordinary kriging in tibetan plateau. *Ecological Indicators*, 45:184–194, 2014.
- Eric A Davidson, Susan E Trumbore, and Ronald Amundson. Biogeochemistry: soil warming and organic carbon content. *Nature*, 408(6814):789–790, 2000.
- Anthony Christopher Davison and David Victor Hinkley. *Bootstrap methods and their application*, volume 1. Cambridge university press, 1997.
- M Fantappiè, G LAbate, and EAC Costantini. Factors influencing soil organic carbon stock variations in italy during the last three decades. In *Land degradation and desertification: assessment, mitigation and remediation*, pages 435–465. Springer, 2010.
- FAO. Food and agriculture organization of the united nations, rome, italy. In *Global Symposium on Soil Organic Carbon*, 2017.
- Roberta Farina, Alessandro Marchetti, Rosa Francaviglia, Rosario Napoli, and Claudia Di Bene. Modeling regional soil c stocks and co₂ emissions under mediterranean cropping systems and soil types. *Agriculture, Ecosystems & Environment*, 238:128–141, 2017.
- Rosina Grimm, T Behrens, Michael Märker, and Helmut Elsenbeer. Soil organic carbon concentrations and stocks on barro colorado islanddigital soil mapping using random forests analysis. *Geoderma*, 146(1):102–113, 2008.
- Clovis Grinand, Gueric Le Maire, Ghislain Vieilledent, H Razakamanarivo, Tiana Razafimbelo, and Martial Bernoux. Estimating temporal changes in soil carbon stocks at ecoregional scale in madagascar using remote-sensing. *International Journal of Applied Earth Observation and Geoinformation*, 54:1–14, 2017.

- IUSS Working Group et al. World reference base for soil resources 2014 international soil classification system for naming soils and creating legends for soil maps. *FAO, Rome*, 2014.
- Brent L Henderson, Elisabeth N Bui, Christopher J Moran, and DAP Simon. Australia-wide predictions of soil properties using decision trees. *Geoderma*, 124(3):383–398, 2005.
- Tomislav Hengl, Jorge Mendes de Jesus, Robert A MacMillan, Niels H Batjes, Gerard BM Heuvelink, Eloi Ribeiro, Alessandro Samuel-Rosa, Bas Kempen, Johan GB Leenaars, Markus G Walsh, et al. Soilgrids1kmglobal soil information based on automated mapping. *PLoS One*, 9(8):e105992, 2014.
- Roland Hiederer and Martin Köchy. Global soil organic carbon estimates and the harmonized world soil database. *EUR*, 79:25225, 2011.
- Eleanor U Hobley, Jeff Baldock, and Brian Wilson. Environmental and human influences on organic carbon fractions down the soil profile. *Agriculture, Ecosystems & Environment*, 223:152–166, 2016.
- U Hoffmann, T Hoffmann, G Jurasinski, S Glatzel, and NJ Kuhn. Assessing the spatial variability of soil organic carbon stocks in an alpine setting (grindelwald, swiss alps). *Geoderma*, 232:270–283, 2014.
- Ni Huang, Li Wang, Yiqiang Guo, Pengyu Hao, and Zheng Niu. Modeling spatial patterns of soil respiration in maize fields from vegetation and soil property factors with the use of remote sensing and geographical information system. *PloS one*, 9(8):e105150, 2014.
- Radoslaw Kaczynski, Grzegorz Siebielec, Marjoleine C Hanegraaf, and Hein Korevaar. Modelling soil carbon trends for agriculture development scenarios at regional level. *Geoderma*, 286:104–115, 2017.
- Roger Koenker. Quantile regression, 2005.
- Roger Koenker and Gilbert Bassett Jr. Regression quantiles. *Econometrica: journal of the Econometric Society*, pages 33–50, 1978.
- Marine Lacoste, Budiman Minasny, Alex McBratney, Didier Michot, Valérie Viaud, and Christian Walter. High resolution 3d mapping of soil organic carbon in a heterogeneous agricultural landscape. *Geoderma*, 213:296–311, 2014.
- Emanuele Lugato, Panos Panagos, Francesca Bampa, Arwyn Jones, and Luca Montanarella. A new baseline of organic carbon stock in european agricultural soils using a modelling approach. *Global change biology*, 20(1):313–326, 2014.
- M v Lützw, Ingrid Kögel-Knabner, K Ekschmitt, E Matzner, G Guggenberger, B Marschner, and H Flessa. Stabilization of organic matter in temperate soils: mechanisms and their relevance under different soil conditions—a review. *European Journal of Soil Science*, 57(4):426–445, 2006.

- J Meersmans, F De Ridder, Frank Canters, Sarah De Baets, and Marc Van Molle. A multiple regression approach to assess the spatial distribution of soil organic carbon (soc) at the regional scale (flanders, belgium). *Geoderma*, 143(1):1–13, 2008.
- Bradley A Miller, Sylvia Koszinski, Wilfried Hierold, Helmut Rogasik, Boris Schröder, Kristof Van Oost, Marc Wehrhan, and Michael Sommer. Towards mapping soil carbon landscapes: Issues of sampling scale and transferability. *Soil and Tillage Research*, 156: 194–208, 2016.
- Arun Mondal, Deepak Khare, and Sananda Kundu. Impact assessment of climate change on future soil erosion and soc loss. *Natural Hazards*, 82(3):1515–1539, 2016.
- Antonios Morellos, Xanthoula-Eirini Pantazi, Dimitrios Moshou, Thomas Alexandridis, Rebecca Whetton, Georgios Tziotzios, Jens Wiebenson, Ralf Bill, and Abdul M Mouazen. Machine learning based prediction of soil total nitrogen, organic carbon and moisture content by using vis-nir spectroscopy. *Biosystems Engineering*, 152:104–116, 2016.
- VL Mulder, M Lacoste, AC Richer-de Forges, MP Martin, and D Arrouays. National versus global modelling the 3d distribution of soil organic carbon in mainland france. *Geoderma*, 263:16–34, 2016.
- Miriam Muñoz-Rojas, A Jordán, LM Zavala, FA González-Peñaloza, D De la Rosa, Rafael Pino-Mejias, and María Anaya-Romero. Modelling soil organic carbon stocks in global change scenarios: a carbo soil application. *Biogeosciences*, 10(12):8253, 2013.
- M Nussbaum, A Papritz, A Baltensweiler, and L Walthert. Estimating soil organic carbon stocks of swiss forest soils by robust external-drift kriging. *Geoscientific Model Development*, 7(3):1197–1210, 2014.
- Kenneth R Olson, Mahdi Al-Kaisi, Rattan Lal, and Larry Cihacek. Impact of soil erosion on soil organic carbon stocks. *Journal of Soil and Water Conservation*, 71(3):61A–67A, 2016.
- Panos Panagos, Cristiano Ballabio, Katrin Meusburger, Jonathan Spinoni, Christine Alewell, and Pasquale Borrelli. Towards estimates of future rainfall erosivity in europe based on redes and worldclim datasets. *Journal of Hydrology*, 548:251–262, 2017.
- William J Parton, J WB Stewart, and C Vernon Cole. Dynamics of c, n, p and s in grassland soils: a model. *Biogeochemistry*, 5(1):109–131, 1988.
- S Pellegrini, N Vignozzi, EAC Costantini, and G LAbate. A new pedotransfer function for estimating soil bulk density. In *Changing soils in a changing world: the soils of tomorrow. Book of abstracts. 5th International congress of European society for soil conservation, Palermo*, pages 25–30, 2007.
- Yi Peng, Xiong Xiong, Kabindra Adhikari, Maria Knadel, Sabine Grunwald, and Mogens Humlekrog Greve. Modeling soil organic carbon at regional scale by combining multi-spectral images with laboratory spectra. *PloS one*, 10(11):e0142295, 2015.

- Bruce C Pengelly and Brigitte L Maass. Lablab purpureus (L.) sweet-diversity, potential use and determination of a core collection of this multi-purpose tropical legume. *Genetic Resources and Crop Evolution*, 48(3):261–272, 2001.
- Chiara Piccini, Alessandro Marchetti, and Rosa Francaviglia. Estimation of soil organic matter by geostatistical methods: Use of auxiliary information in agricultural and environmental assessment. *Ecological Indicators*, 36:301–314, 2014.
- RR Ratnayake, T Kugendren, and N Gnanavelrajah. Changes in soil carbon stocks under different agricultural management practices in north sri lanka. *Journal of the National Science Foundation of Sri Lanka*, 42(1), 2014.
- Arjan Reijneveld, Joke van Wensem, and Oene Oenema. Soil organic carbon contents of agricultural land in the netherlands between 1984 and 2004. *Geoderma*, 152(3):231–238, 2009.
- Luis Rodríguez-Lado and Antonio Martínez-Cortizas. Modelling and mapping organic carbon content of topsoils in an atlantic area of southwestern europe (galicia, nw-spain). *Geoderma*, 245:65–73, 2015.
- Raphael A Viscarra Rossel and Johan Bouma. Soil sensing: A new paradigm for agriculture. *Agricultural Systems*, 148:71–74, 2016.
- Gustavo Saiz, Michael I Bird, Tomas Domingues, Franziska Schrodtt, Michael Schwarz, Ted R Feldpausch, Elmar Veenendaal, Gloria Djagbletey, Fidele Hien, Halidou Compaore, et al. Variation in soil carbon stocks and their determinants across a precipitation gradient in west africa. *Global change biology*, 18(5):1670–1683, 2012.
- Claude Sammut and Geoffrey I. Webb, editors. *Leave-One-Out Cross-Validation*, pages 600–601. Springer US, Boston, MA, 2010. ISBN 978-0-387-30164-8. doi: 10.1007/978-0-387-30164-8_469.
- Calogero Schillaci, Marco Acutis, Luigi Lombardo, Aldo Lipani, Maria Fantappiè, Michael Märker, and Sergio Saia. Spatio-temporal topsoil organic carbon mapping of a semi-arid mediterranean region: The role of land use, soil texture, topographic indices and the influence of remote sensing data to modelling. *Science of The Total Environment*, 601: 821–832, 2017a.
- Calogero Schillaci, Luigi Lombardo, Sergio Saia, Maria Fantappiè, Michael Märker, and Marco Acutis. Modelling the topsoil carbon stock of agricultural lands with the stochastic gradient treeboost in a semi-arid mediterranean region. *Geoderma*, 286:35–45, 2017b.
- Carlos A Sierra, Susan E Trumbore, Eric A Davidson, Sara Vicca, and I Janssens. Sensitivity of decomposition rates of soil organic matter with respect to simultaneous changes in temperature and moisture. *Journal of Advances in Modeling Earth Systems*, 7(1):335–356, 2015.

- Kandrika Sreenivas, VK Dadhwal, Suresh Kumar, G Sri Harsha, Tarik Mitran, G Sujatha, G Janaki Rama Suresh, MA Fyzee, and T Ravisankar. Digital mapping of soil organic and inorganic carbon status in india. *Geoderma*, 269:160–173, 2016.
- R Taghizadeh-Mehrjardi, K Nabiollahi, and R Kerry. Digital mapping of soil organic carbon at multiple depths using different data mining techniques in baneh region, iran. *Geoderma*, 266:98–110, 2016.
- Zheng Tian, Xiuqin Wu, Erfu Dai, and Dongsheng Zhao. Soc storage and potential of grasslands from 2000 to 2012 in central and eastern inner mongolia, china. *Journal of Arid Land*, 8(3):364–374, 2016.
- José Luis Vicente-Vicente, Roberto García-Ruiz, Rosa Francaviglia, Eduardo Aguilera, and Pete Smith. Soil carbon sequestration rates under mediterranean woody crops using recommended management practices: a meta-analysis. *Agriculture, Ecosystems & Environment*, 235:204–214, 2016.
- Tristram O West and Mohan K Wali. Modeling regional carbon dynamics and soil erosion in disturbed and rehabilitated ecosystems as affected by land use and climate. *Water, Air, & Soil Pollution*, 138(1):141–164, 2002.
- Yusuf Yigini and Panos Panagos. Assessment of soil organic carbon stocks under future climate and land cover changes in europe. *Science of the Total Environment*, 557:838–850, 2016.
- Yang Yu, David Makowski, Tjeerd Jan Stomph, and Wopke van der Werf. Robust increases of land equivalent ratio with temporal niche differentiation: A meta-quantile regression. *Agronomy Journal*, 108(6):2269–2279, 2016. doi: 10.2134/agronj2016.03.0170.